Studying the properties of prepared kaolin/epoxy nanocomposites for flame retardancy

M. T. Abd and I. N. Kashkool

Bilad Al Rafidain University, College of Medical and Health Technology, Iraq.

Saif Khalel Jasim

Ministry of Education. Diyala Education Directorate, Diyala, Iraq.
e-mail: saifalaosy@gmail.com

Received 12 November 2025; accepted 8 June 2026

Numerous everyday goods, including fabrics, electrical appliances, vehicles, and airplanes, are currently undergoing extensive testing and inspection for their flammability features. The results of the study showed that adding 10% by weight of nano-kaolin achieved the best flame resistance performance, recording the highest limiting oxygen index (LOI) and lowest rate of burn (RB) compared to pure epoxy, indicating the formation of an effective insulating char layer. By lowering the total fire risk associated with the use of highly flammable raw materials in goods such as textiles, apparel, composites, and plastics, flame retardants perform a critical protective role in preserving lives and property. In this study, kaolin and epoxy were used to prepare a nanocomposite flame retardant. The used kaolin was tested by X-ray diffraction and (AFM) tests. The results showed that the powders possess multi-phases (presence of quartz and goethite phases alongside kaolinite) and also have a mean grain size of (38 nm) according to AFM results showing a homogeneous distribution of particles and root mean square (RMS) of (12.25). Also, the energy-dispersive spectroscopy analysis (EDX) showed that the presence of the essential elements (Al, Si, O) plus trace amounts of Fe and Ti of these powders was accurate and clear. The nanocomposites were prepared by mixing the kaolin nanopowder with the epoxy resin by weight percentages of (2, 4, 6, 8 and 10%). To determine the efficiency of these additives in flame retardants and to increase the combustion resistance of epoxy resin, different methods of measurement were used according to ASTM, average time of burning, average extent of burning, rate of burning, limiting oxygen index, maximum flame height and residue percentage succeeding combustion. Based flame retardant are commercially successful and they are more environmentally friendly as compared to halogenated and non-halogenated inorganic or organic types and they are being applied suitably with a crossinker and/or binder copolymer that makes the FRs more resistant to common weathering conditions and exposures. They also produce less or no obnoxious gases while burning.

Keywords: Flame Retardant; flammability properties; kaolin; limiting oxygen index; rate of burning.

DOI: https://doi.org/10.31349/RevMexFis.72.061003

1. Introduction

Flammable materials, such as polymers, that are used in a variety of aspects of human life pose a significant fire hazard. Flame retardants help to mitigate this risk while also assisting in the achievement of reasonable amounts of fire prevention [1,2]. There are advantages and disadvantages to each of these substances that have been in use for a long time [3]. It is dependent on a variety of factors as to how effective they are at attempting to reduce the flammability of various materials [4]. It can be said that these factors are material type, the application and the environment, which is the main container for these materials and applications [5,6]. The second factor is the compatibility/compliance of a flame retardant with a particular substance, as well as, the third factor is methodologies for processing [7,8]. When burned, some flame retardants produce toxic gases in space, and others can cause the premature degradation of some materials [9,10]. The hydrolysis of the product may be caused by some of them, which are hygroscopic [2]. When it comes to being effective, some fire retardants must be used in large quantities, which results in deterioration of mechanical properties as well as a decrease in interfacial adhesion between different components of the composite [11,12].

Nanoclays are receiving a lot of attention these days for their ability to act as fire-resistant added chemicals. Inorganic clay-based nanomaterials with the ability to integrate with a wide range of materials belong to this category [13]. Many minerals, such as hectorite, montmorillonite (MMT), kaolinite, halloysite, and bentonite, form silicate and perhaps aluminum-silicate constructions [14].

Nanoclays, with the exception of traditional flame retardants, are environmentally friendly, highly effective, and, most importantly, could indeed convey unique characteristics to a material [15]. The use of nanoclays in resins, such as MMT, has been shown to reduce flammability while also improving strength properties [16]. Tiny particles also make it harder for carbon chains to move around, which changes the nanocomposites' volume, surface, and characteristics [5].

Among nanoclays used to make UPRs, MMT is among the most commonly used ones. They are very big. It has a big surface area and a lot of space between the longest and

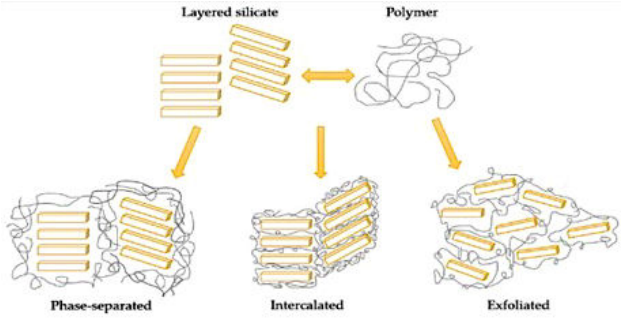


FIGURE 1. A scheme of dispersion states of the clay in the polymer matrix [6].

the smallest parts [8]. This improves the fire retardancy of the material, but only if the material is spread out well. A decrease in the specific surface area, on the other hand, may result in a reduction in the flame retardant attributes. It's possible to have the clay in one of three different dispersion states: phase-separation, intercalation, or exfoliation. As a result of its larger specific surface area, the last option is preferred. Figure 1 depicts all of the forms.

Since nanoclays have such a large surface area, they can decrease the amount of admixture by as much as a few percent. The mechanism of action is based on the formation of a char layer, which prevents heat transfer. In Ref. [7], it was shown that capturing free radicals is a common phenomenon for inorganic nanoclays. After being exposed to high temperatures, nanocomposites that included silicates or silica retain their structural integrity, and the decomposition of organic components takes place within the material, cutting the level of soot issued [8]. The accumulation of a carbonaceous-silicate char layer on the surface of the material results in the insulation of the material and the retardation of mass loss. By enhancing char formation and decreasing heat release, nano flame retardants have been found to reduce flammability as it was shown in Ref. [9].

The physical preparation method seems to be more productive if silicate layers of nanoclays are properly intercalated or exfoliated in the matrix. A labyrinth effect occurs when volatile species released during combustion are unable to diffuse freely because of the tortuous path formed by these layers [16,17].

2. Experimental

This part discusses the practical steps involved in preparing the materials used in flame retardant specimens' preparation, functionalization of kaolinite and preparation of the kaolin/epoxy resin nanocomposites.

2.1. Materials

Imported from the Sikadur-52 company in the United States, epoxy resin and hardener type (amine). For curing, this study used a 2:1 ratio of epoxy and hardener. The raw kaolinite was obtained from white stone produced and processed in the western desert mining division/Al-Rutbah/Al-Anbar governorate/ Iraq, with the chemical formula of $Al_2Si_2O_5(OH)_4$.

Functionalization of kaolinite: The kaolin nanopowder was prepared from its raw stones, which were crashed and grinded to obtain powders with a final fineness of fewer than 20 μm and used for size reduction, mixing and triturating. The kaolin nanoparticle was prepared by mixing (30 g) of ultra-fine powder with (300 mL) of ethanol, (100 mL) of distilled water and (10 mL) of HCl with a concentration of (36.5%). After stirring for 14 hours, the mixture was filtered and washed several times by using distilled water to get rid of the effects of HCl. The importance of using HCl lies in activating the kaolin surface and removing carbonate impurities, thereby increasing its compatibility with epoxy resin. The solution containing the mixture was tested using the pH meter to confirm its equivalence then filtered, dried in air at room temperature and calcinated at 800 °C for 4 hours. To convert it into the chemically active form metacacoline. To remove the impurities which present in the powder. AFM, XRD and EDX tests were performed to prove the particle size of prepared powder on the nanoscale.

Pre-processing of the kaolin/epoxy resin nanocomposites: Hand lay-up molding was used to prepare the nanocomposites, to ensure effective dispersion and prevent agglomeration at high concentrations, intensive mechanical mixing was used to increase the penetration of polymer chains between the nanolayers. Molded cases in the form of sheets with sizes of $13 \times 13 \times 0.4$ cm^3. All samples were given sufficient time to harden (24 hours) to ensure that the chemical reaction in the presence of nanoparticles was complete. These epoxy resin sheets were made for each percentage weight of flame retardant substance (kaolin) nanopowder (0, 2, 4, 6, 8, and 10) wt. percent, respectively. Depending on the method of test, the samples were laser cut and obtained charming ends. The samples were chosen as 130 ± 5 mm for the limiting oxygen index (LOI) length, the height of flame (HF) length is equal to 125 ± 5 mm, and with the rate of burning (RB) length matches the LOI length. That is, the width of LOI was 6.5 ± 0.5 mm with a width of 10 ± 0.1 mm for the HF, while RB with set to 12.5 ± 0.5 mm. Furthermore, their thickness was equal to 3.0 ± 0.1 mm, as shown in Figure (2). It should be noted that the diagram shown in Fig. 2 represents an illustrative model of the mechanism of chemical interaction and bonding, where the step of 'silane grafting' in the diagram reflects the principle of surface activation achieved in this study

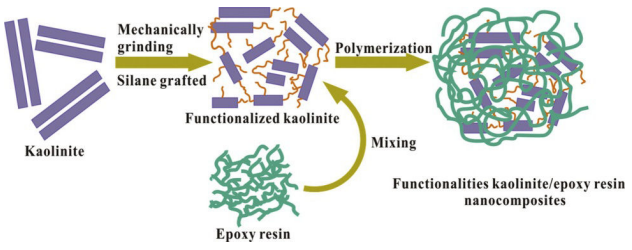


FIGURE 2. Diagram of pre-processing of the kaolin/epoxy resin nanocomposites.

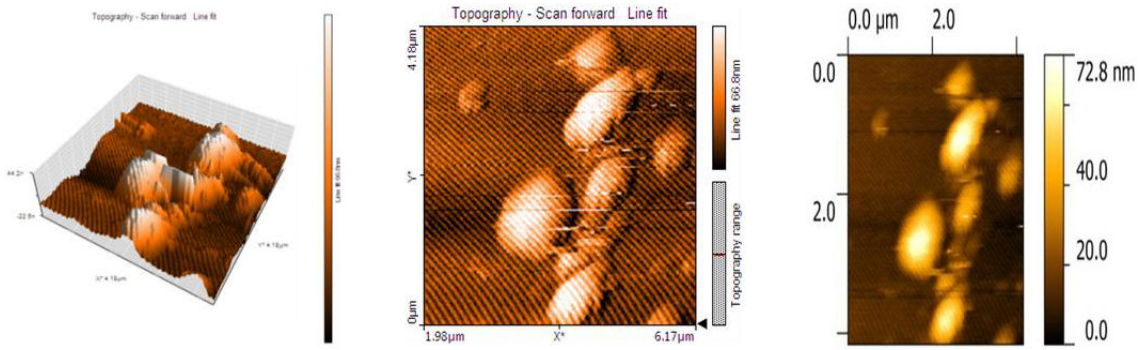


FIGURE 3. The surface topography of kaolin nanopowder.

by activating kaolin with hydrochloric acid (HCl) and calcining at 800 °C, which created strong and highly compatible bonds between the nanoparticles and the epoxy matrix.

Characterization: The acidity and alkalinity of the solution containing kaolin powder were measured individually by using the pH meter type (pH starer 2000). The surface topography of the prepared nanopowder was studied by using a German-made compact AFM. The crystalline structure of the prepared powder was identified by using X-ray diffraction type (Shimadzu XRD-6000) with the target (Cu) and wavelength (1.5406 Å). The chemical composition of the prepared powder was studied using a scanning electron microscope test, model (AIS 2300, USA). In order to determine the flammability of polymers, the limiting oxygen index (LOI), was used (ASTM: D-2863). It is necessary to monitor the RB, the average time of burning (ATB) and the average extent of burning (AEB) in accordance with (ASTM: D-635). While HF and the quantity of weight loss in the polymer are carried out in compliance with the scheme (ASTM: D-3014).

3. Result and discussion

3.1. PH meter test

The acidity and alkalinity for the solution of the nanopowder were measured, where kaolin solution has neutral PH.

3.2. Atomic force microscopy test

Surface morphology of prepared kaolin nanopowder image is illustrated in Fig. 3, where the particles appear with clear nanoscale dimensions and an average size of 38 nanometres, with peak heights reaching approximately 72.8 nanometres, which enhances the contact surface area between the nano and polymer.

TABLE I. Values of surface roughness, RMS and mean grain size of prepared powder.

Sample	Surface Roughness (nm)	RMS (nm)	Mean grain Size (nm)
Kaolin	12.251	8.5356	38

3.3. X-ray diffraction-test

From Table I, it was observed that the surface roughness and mean grain size of the preparation due to the large size of grain causes porosity during the molding, which is considered a weak area of the sample because it will be a store of oxygen. From Fig. 4, there are three phases are detected in the XRD pattern: kaolinite, goethite and quartz with crystalline phases triclinic, orthorhombic and hexagonal, respectively [18,19]. The average grain size for synthesized kaolin was determined by Scherrer's equation. It was found to be about (42.7 nm). This result is in full agreement with the results that were obtained in Table I.

3.4. Energy dispersive X-ray spectroscopy-test

The elemental composition in the reaction mixture of nanopowder material was analyzed by detecting X-ray emission due to the electron beam where the energy distribution of the X-ray emission was analyzed by (EDX). The EDX spectrum of raw material and prepared nanopowder and kaolin

TABLE II. XRD data of prepared nano-powder for the strongest three peaks.

Sample	$2\theta(^\circ)$	d(Å)	FWHM(°)
Kaolin	26.5912	3.34949	0.17050
	20.8054	4.26604	0.20240
	50.0568	1.82075	0.16990

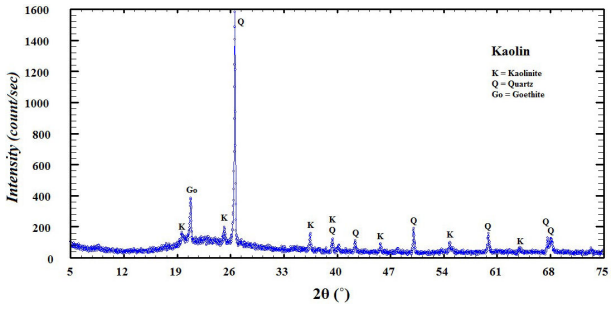


FIGURE 4. XRD pattern of kaolin nanopowder.

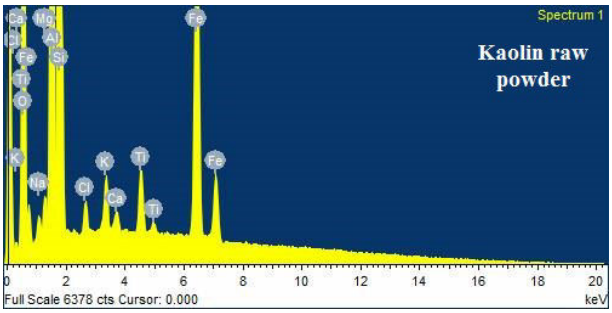


FIGURE 5. EDX spectrum of kaolin raw powder.

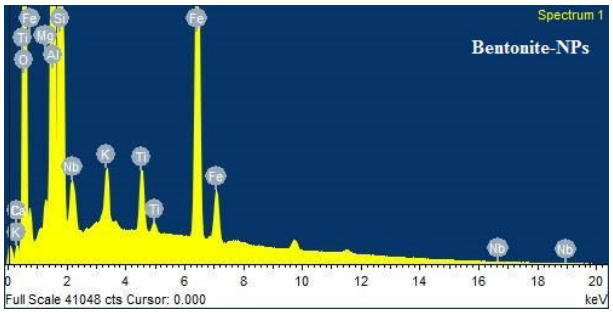


FIGURE 6. EDX spectrum of kaolin nanopowder.

TABLE III. Chemical composition of kaolin raw powder.

Element	Weight%	Atomic %	Series
O	52.52	69.81	K
Mg	0.47	0.41	K
Al	12.64	9.96	K
Ca	0.26	0.14	K
Si	16.43	12.44	K
K	0.63	0.34	K
Ti	1.17	0.52	K
Fe	15.02	5.72	K
Na	0.47	0.44	K
Cl	0.39	0.22	K

TABLE IV. Chemical composition of kaolin nanopowder.

Element	Weight %	Atomic %	Series
O	51.95	67.47	K
Al	20.28	15.62	K
Si	19.38	14.34	K
K	0.79	0.42	K
Ti	0.89	0.39	K
Fe	1.75	0.65	K
Nb	4.96	1.11	L

shows in Figs. 5 and 6, respectively. The elements that constitute the raw material and prepared nanopowder are given in atomic and mass percentages in Tables III and IV, respectively. From Fig. 6, the kaolin nanopowder is composed mainly of Al_2O_3 and SiO_2, elements Al, Si, O , this result confirms that the kaolin clay is mainly composed of kaolinite and quartz clay minerals. Trace amounts of iron and titanium were also detected as natural impurities in the ore structure, this corresponds to the result of XRD. In the clay powder, (Al_2O_3) doesn't exist in its free form but is bound to the clay minerals.

3.5. LOI-test (limiting oxygen index)

The limiting oxygen index (LOI) model is the most commonly used method for determining the resistance to ignition and comparative flammability of polymeric materials. It was determined using the (ASTM: D-2863), and the results were determined by using the formula [20,21]:

$$n\% = \frac{V_{O_2}}{V_{O_2} + V_{N_2}} \times 100, \tag{1}$$

where $n\%$ stands for LOI, the volumetric speed flow of nitrogen in ml/sec is represented by V_{N_2}, while V_{O_2} refers to the volumetric speed of oxygen in ml/sec.

Table V shows the outcomes that were obtained. That is, in Table V, it is shown that LOI is increased when the reinforcement ratios of the added kaolin nanopowder to the epoxy (directly proportional) increase. This is due to the fact that these additives create an inert atmosphere, which diminishes and hinders the oxygen from getting to the flame zone, which really is essential to sustaining the ignition's stability.

As a result of the exposure of (kaolin/Epoxy) nanocomposites in the air and at atmospheric pressure, dehydroxylation occurs by an endothermic process at (550-700°C) to give a meta form called irregular metakaolin and a continuous loss of hydroxyl groups (OH^-) at temperatures (700-800°C), due to oxolation. Removal of hydroxyl from kaolin leads to a failure of the material and thus non-resistance to flame [22,23]. Kaolin works by heat absorption mechanism and cools the surface of the material to 700°C.

3.6. Burning rate-test

The test was measured using the (ASTM: D-635) manner and intended to use formula (2) and (3), [24,25], ATB in minutes and AEB were calculated as follows:

$$ATB = \frac{\sum(t-30)}{N}, \tag{2}$$

$$ABE = \frac{\sum(100-X)}{N}. \tag{3}$$

TABLE V. Results of LOI for the epoxy without and with reinforcement ratio of kaolin nanopowder.

Type of additive	LOI vs. Additives%					
	0	2	4	6	8	10
Neat Epoxy	19.59	-	-	-	-	-
Epoxy + Kaolin	-	20.23	21.1	21.56	21.95	22.33

TABLE VI. ATB, AEB, RB, SE and NB for epoxy without and with reinforcement ratios of kaolin nanopowder.

Test	Additives %					
	Original	2	4	6	8	10
ATB	5.35	5.81	6.08	6.9	4.5	3.61
AEB	10.3	10.3	10.3	10.3	4.12	3.88
RB	1.92	2.02	1.91	1.83	1.65	1.34
SE	-	-	-	-	-	-
NB	-	-	-	-	-	-

In the last two expressions, the time in minutes is represented by t, when self-extinguishing occurs, the length of the not yet burned portion of the structure is evaluated in cm, which is represented by X, and N is the number of samples. A worthy mention here is that according to the (ASTM: D-635) methodology, RB is measured in cm/min. Moreover, the self-extinguishing is abbreviated by SE and NB stands for that after removing the heat source, the specimen's ignition does not continue.

The results of RB of epoxy with additive show a large drop in RB. The RB of epoxy samples was measured without and with additive in addition to the values of (ATB) and (AEB) were calculated by using Eqs. (2) and (3), respectively, as listed in Table VI. The decrease in the R.B is inversely relative to the growth in the reinforcement ratios of the added additive to the epoxy for the same reason mentioned in the LOI test.

3.7. HF maximum-test

The burning substantial residual weight percentage was determined using the strategy defined in (ASTM: D-3014) and determined by calculating using the equation given [25,26]:

$$PWR\% = \frac{W_1 - W_2}{W_1} \times 100. \tag{4}$$

In which, the weight of the specimen before combustion in gm is represented by W_1, W_2 stands for the weight of residual material succeeding the combustion also in gm, furthermore, PWR% is the residual percentage weight of the burning material.

Table VII summarizes the output of the HF measurement for EP including several kaolin weight proportions. The results showed that the increasing reinforcement ratios of the added additive lead to the decrease of (HF) (inversely proportional) and an increase in the effectiveness and retardancy (directly proportional) for the same reason mentioned in the LOI test.

TABLE VII. (HF) with reinforcement ratios of kaolin.

Test	H vs. percentage additives					
	Non	2	4	6	8	10
W1(gm)	4.56	4.76	4.85	5.23	5.31	5.36
W2(gm)	1.37	0.8	0.86	1.28	1.4	1.47
PWR%	69.95	83.19	82.26	75.52	73.63	72.57
HF(cm)	12.3	11.3	8.8	7.43	5.44	4.52

TABLE VIII. ATB, AEB, RB, SE and NB for EP.

Test	Additives %					
	Non	2	4	6	8	10
ATB	5.35	6.71	7.3	3.22	2.52	2.25
AEB	10.3	10.3	10.3	4.1	1.8	1.4
RB	1.92	1.73	1.69	1.2	0.57	0.49
SE	-	-	-	Yes	Yes	Yes
NB	-	-	-	-	-	-

4. Conclusions

The nanocomposites of functionalized kaolin/epoxy resin were synthesized using synthesized kaolin as padding. The used method was successful in preparing nanopowder for kaolin clay with an average grain size (38 nm). Limiting oxygen index (LOI) was increased and rate of burning (R.B) and maximum flame height (HF) were decreased for epoxy resin by increasing the reinforcement ratios of additive. They demonstrated that surface functionalization of kaolin is a straightforward but effective technique for producing elevated clay mineral-polymer nanocomposites.

Acknowledgment

The authors would like to thank the University of Diyala/College of Science/Department of Physics for the technical support to complete this work in their laboratories.

1. Y. Wang, T. Henriksen, M. Deo, and R. A. Mentzer, Factors contributing to US chemical plant process safety incidents from 2010 to 2020, *J. Loss Prev. Process Ind.* **71** (2021) 104512. https://doi.org/10.1016/j.jlp.2021.104512

2. S. S. Abdullah and F. L. Ahmed, Structural and optical studies on sliver nitrate doped polymer blend and effect on some pathogenic bacteria, *Rev. Mex. Fis.* **71** (2025) 041004. https://doi.org/10.30723/ijp.v19i49.625

3. S. Sonkaria and H. J. Kim, Nanoscale configuration of clay-interlayer chemistry: A precursor to enhancing flame retardant properties, *IntechOpen* (2021) 75385. https://www.intechopen.com/chapters/75385

4. T. Y. Sabri, S. K. Jasim, A. A. Habeeb, and A. S. Jasim, Preparation and Study Ag Nanoparticles via PLAL Tech-

nique: Influence of Different Number of Pulses, *Int. J. Nanoelectron. Mater*. **17** (2024) 45. https://doi.org/10.58915/ijneam.v17i1.458

5. S. K. Jasim, A. M. Shano, and S. K. Adnan, Zinc Oxide Poly Crystals Heterojunction and Infrared-Blind UV-Photodetector, *J. Nano- Electron. Phys*. **16** (2024) 01012. https://doi.org/10.21272/jnep.16(1).01012
6. K. Zheng, F. Zheng, J. Lin, Z. Ren, and Y. Lin, Utilization of red mud as copper substitute in eco-friendly resin-based brake composites: Performance evaluation and machine learning prediction, *Tribol. Int*. **214** (2026) 111324. https://doi.org/10.1016/j.triboint.2025.111324
7. N. Abu-Thabit *et al*., Preparation of pH-Indicative and Flame-Retardant Nanocomposite Films for Smart Packaging Applications, *Sensors* **20** (2020) 5462. https://doi.org/10.3390/s20195462
8. S. K. Jasim, W. M. W. A. Kamil, A. A. Habeeb, and E. Ali, Effect of Cinnamon Nano/Micro Particles at Antibacterial Activity, *J. Phys. Sci*. **36** (2025) 43. https://doi.org/10.21315/jps2025.36.3.4
9. G. Jin *et al*., A novel coarse-grained discrete element method for simulating failure process of strongly bonded particle materials, *Powder Technol*. **464** (2025) 121212. https://doi.org/10.1016/j.powtec.2025.121212
10. S. K. Jasim, S. M. A. Al Hussan, and M. T. Abd, Improving the Mechanical Properties of Dental Fillings by Adding TiO_2 NPs Prepared Laser Ablation, *Bio. Nano. Science* **15** (2025) 330. https://doi.org/10.1007/s12668-025-01970-y
11. S. K. Jasim, S. M. A. A. Hussan, A. S. Noori, and A. A. Habeb, Determine surface plasmon resonance and effect parameters laser ablation on Cu and Zn nanoparticles, *AIP Conf. Proc.* **3219** (2024) 060008. https://doi.org/10.1063/5.0236469
12. X. Li and Ma, Z., Inherent anisotropy of aeolian sand with different bedding angles in true-triaxial tests, *Eng. Geol.* **356** (2025) 108272. https://doi.org/10.1016/j.enggeo.2025.108272
13. F. Xu *et al*., Novel high-efficiency casein-based P-N-containing flame retardants with multiple reactive groups for cotton fabrics, *ACS Sustainable Chem. Eng.* **7** (2019) 13999. https://doi.org/10.1021/acssuschemeng.9b02474
14. B. M. Dheyaa, W. H. Jassim, and N. A. Hameed, Evaluation of the epoxy/antimony trioxide nanocomposites as flame retardant, *J. Phys. Conf. Ser*. **1003** (2018) 012078. https://doi.org/10.1088/1742-6596/1003/1/012078
15. L. Su, X. Zeng, H. He, Q. Tao, and S. Komarneni, Preparation of functionalized kaolinite/epoxy resin nanocomposites with enhanced thermal properties, *Appl. Clay Sci*. **148** (2017) 103. https://doi.org/10.1016/j.clay.2017.08.017
16. Z. Luo *et al*., Synergistic enhancement of heat resistance and mechanical performance of epoxy resin by introducing entanglement effect, *Composites Part A* **203** (2026) 109581. https://doi.org/10.1016/j.compositesa.2026.109581
17. S. A. Zaidan and M. H. Omar, The effects of bauxite, metakaolin, and porosity on the thermal properties of prepared Iraqi clays refractory mortars, *Appl. Phys. A* **124** (2018) 386. https://doi.org/10.1007/s00339-018-1759-2
18. C. Liu *et al*., Phosphorous-Nitrogen Modification of Epoxy Grafted Poly-Acrylic Resin: Synergistic Flame Retardment Effect, *Polymers* **13** (2021) 2826. https://doi.org/10.3390/polym13162826
19. X. S. Wang, G. L. Xu, Y. Wang, Y. Liang, and J. Hu, Preparation of phosphorus-containing poly-acrylate resins and their flame resistant properties, *J. Chem. Eng. Chin. Univ*. **31** (2017) 186. http://dx.doi.org/10.3969/j.issn.1003-9015.2017.01.026
20. A. H. Ahmed, A. S. Jasima, and S. K. Jasim, Synthesis of Gold Nanoparticles by Pulsed Laser Ablation and its Study Physical and Mechanical Properties, *Int. J. Nanoelectron. Mater*. **17** (2024) 1465. https://doi.org/10.58915/ijneam.v17i4.1465
21. N. R. Kopparthi, J. Schuster, and Y. P. Shaik, Fabrication and Characterization of Bamboo-Epoxy Reinforced Composite for Thermal Insulation, *Open J. Compos. Mater.* **14** (2023) 15. https://doi.org/10.4236/ojcm.2024.141002
22. H. Ma *et al*., Multifunctional Graphite Nanosheet-Hydrophilic Epoxy Anticorrosion Coatings via Size Confinement of Exfoliated Graphite, *Polymers* **17** (2025) 1803. https://doi.org/10.3390/polym17131803
23. C. Yan *et al*., Additive manufacturing of hydroxyapatite and its composite materials: A review, *J. Micromech. Mol. Phys.* **5** (2020) 2030002. https://doi.org/10.1142/S2424913020300029
24. F. Heidari, M. Razavi, M. A. A. Zamani, M. Tahriri, and L. Tayebi, A comparison between the properties of natural hydroxyapatite produced by cold isostatic pressing and spark plasma sintering techniques, *J. Aust. Ceram. Soc.* **54** (2018) 337. https://doi.org/10.1007/s41779-017-0158-z
25. Y. Zheng and B. A. Baudet, Pore structure response of reconstituted kaolin and illite-smectite mixed-layer rich clay to 1D compression, *Appl. Clay Sci*. **276** (2025) 107892. https://doi.org/10.1016/j.clay.2025.107892
26. M. Altaf, M. N. Ahmed, A. Iqbal, and A. A. Khan, Synthesis and characterization of novel organoclay-epoxy based flame retardant nanocomposites, *J. Reinf. Plast. Compos*. **45** (2026) 32. https://doi.org/10.1177/07316844241272956